HHS Public Access

Author manuscript

Clin Cancer Res. Author manuscript; available in PMC 2016 March 07.

Published in final edited form as:

Clin Cancer Res. 2015 October 15; 21(20): 4630–4641. doi:10.1158/1078-0432.CCR-14-3195.

Macitentan, a dual endothelin receptor antagonist, in combination with temozolomide leads to glioblastoma regression and long-term survival in mice

Sun-Jin Kim[1,6], **Ho Jeong Lee**[1,6], **Mark Seungwook Kim**[1,6], **Hyun Jin Choi**[1], **Junqin He**[1], **Qiuyu Wu**[1], **Kenneth Aldape**[2], **Jeffrey S. Weinberg**[4], **W. K. Alfred Yung**[5], **Charles A. Conrad**[5], **Robert R. Langley**[1], **François Lehembre**[3], **Urs Regenass**[3], and **Isaiah J. Fidler**[1]

[1]Department of Cancer Biology, Metastasis Research Laboratory, University of Texas MD Anderson Cancer Center, Houston, TX [2]Department of Pathology, University of Texas MD Anderson Cancer Center, Houston, TX [3]Actelion Pharmaceuticals, Ltd., Allschwil, Switzerland [4]Department of Neurosurgery, University of Texas MD Anderson Cancer Center, Houston, TX [5]Department of Neuro-Oncology, University of Texas MD Anderson Cancer Center, Houston, TX

Abstract

Purpose—The objective of the study was to determine whether astrocytes and brain endothelial cells protect glioma cells from temozolomide (TMZ) through an endothelin-dependent signaling mechanism and to examine the therapeutic efficacy of the dual endothelin receptor antagonist, macitentan, in orthotopic models of human glioblastoma.

Experimental Design—We evaluated several endothelin receptor antagonists for their ability to inhibit astrocyte- and brain endothelial cell-induced protection of glioma cells from TMZ in chemoprotection assays. We compared survival in nude mice bearing orthotopically implanted LN-229 glioblastomas or TMZ-resistant (LN-229Res and D54^{Res}) glioblastomas that were treated with macitentan, TMZ, or both. Tumor burden was monitored weekly with bioluminescence imaging. The effect of therapy on cell division, apoptosis, tumor-associated vasculature, and pathways associated with cell survival was assessed by immunofluorescent microscopy.

Results—Only dual endothelin receptor antagonism abolished astrocyte- and brain endothelial cell-mediated protection of glioma cells from TMZ. In five independent survival studies, including TMZ-resistant glioblastomas, 46 of 48 (96%) mice treated with macitentan plus TMZ had no evidence of disease (P<0.0001), whereas all mice in other groups died. In another analysis, macitentan plus TMZ therapy was stopped in 16 mice after other groups had died. Only 3 of 16 mice eventually developed recurrent disease, 2 of which responded to additional cycles of macitentan plus TMZ. Macitentan downregulated proteins associated with cell division and survival in glioma cells and associated endothelial cells, which enhanced their sensitivity to TMZ.

Corresponding Author: Isaiah J. Fidler, DVM, PhD, Department of Cancer Biology, Unit 173, The University of Texas MD Anderson Cancer Center, 1515 Holcombe Boulevard, Houston, TX 77030. Phone: 713-792-8580; ifidler@mdanderson.org.

[6]These authors contributed equally to this work

Conflict of Interest: F.L. and U.R. are employees and shareholders of Actelion Pharmaceuticals, Ltd.

Conclusions—Macitentan plus TMZ are well tolerated, produce durable responses, and warrant clinical evaluation in glioblastoma patients.

Keywords

Glioblastoma; endothelin; macitentan; endothelial cell; astrocyte

Introduction

Glioblastoma is a devastating disease characterized by local invasion, microvascular proliferation, and therapeutic resistance (1, 2). The highly infiltrative nature of glioma cells makes complete surgical resection unlikely, and 90% of tumors recur (3). Resistance to alkylating agents via the DNA repair protein O^6-methylguanine-DNA methyltransferase (MGMT) also remains a barrier to the successful treatment of patients with malignant glioma (4). Efforts to control glioblastoma growth by therapeutic targeting of genetic alterations that drive tumor progression have been hampered by the molecular diversity of the disease (5), which is further augmented by chemotherapy (6). No less than four transcriptional subtypes of glioblastoma have been identified (7), and an individual tumor may be maintained by multiple intermixed populations of cells, each with amplification of a different tyrosine kinase receptor (8). Consequently, it is doubtful that targeting a single oncogenic pathway will improve clinical outcomes in a randomly selected patient population. New treatment strategies for glioblastoma are under investigation, including therapies that target tumor vasculature.

High-grade gliomas are among the most angiogenic of all tumors (9). Tumor blood vessels provide a niche for brain cancer stem cells, where signal-releasing endothelial cells promote their renewal (10). Glioma stem cells ensure their blood supply by releasing vascular endothelial growth factor (VEGF) into the microenvironment (11) and by differentiating into endothelial cells (12) and pericytes (13). VEGF promotes glioma vascularization, oxygenation and growth (14), and its hyperpermeabilizing properties contribute to vasogenic edema (15). However, anti-VEGF therapies do not provide a survival benefit for newly diagnosed glioblastoma patients (16) and anti-VEGF treated tumors transition to a resistant, more infiltrative phenotype (17).

Another vasoactive signaling network that merits investigation as a therapeutic target for glioblastoma is the endothelin axis. The endothelin pathway includes three small peptides (ET-1, ET-2 and ET-3), which mediate their activity by binding to two distinct G-protein-coupled receptors, ET_AR and ET_BR (18). Endothelins were originally characterized based on their powerful vasoconstrictor properties (19), but have since been shown to mediate a variety of physiological functions (18, 20). Elevated endothelin signaling has also been implicated in the pathobiology of several disease processes (18), including cancer (21). Depending on the type of tumor under investigation, activation of endothelin signaling has been shown to promote cancer cell proliferation (22), invasion (23), and resistance to apoptosis (24). ET-1 is also a potent endothelial cell mitogen (25) and can amplify expression of other proangiogenic proteins, such as VEGF (26).

ET_AR and ET_BR are heterogeneously expressed on high-grade glioma cells and tumor-associated endothelial cells (27), and recent evidence suggests that inhibition of ET_BR signaling on glioblastoma stem cells leads to cell death (28). Reports indicate that endothelial cells are the primary cellular source of endothelin in the body (18). ET-1 is particularly enriched in glioblastoma-associated endothelial cells, which produce four times more ET-1 than normal brain endothelial cells (29). Endothelin is also overexpressed by reactive astrocytes (30), which are a histopathologic hallmark of primary (31) and secondary brain tumors (32). Recently, we reported that astrocyte- and brain endothelial cell-derived ET-1 reprograms the transcriptomes of breast cancer cells and lung cancer cells to become resistant to chemotherapy (33).

Herein, we examined whether astrocyte- and endothelial cell-dependent protection of high-grade glioma cells from TMZ is mediated by endothelin signaling and tested the therapeutic efficacy of the novel dual endothelin receptor antagonist, macitentan, in orthotopic models of human glioblastoma, alone and in combination with chemotherapy.

Materials and Methods

Cell lines

Human glioblastoma LN-229 cells, murine NIH 3T3 fibroblasts, murine astrocytes (34), and murine brain endothelial cells (35) were maintained as monolayer cultures in a complete Eagle's minimum essential medium (MEM) supplemented with 10% fetal bovine serum (HyClone, Logan, UT), L-glutamine, sodium pyruvate, non-essential amino acids, and penicillin-streptomycin (all from Life Technologies, Grand Island, NY). The human glioblastoma D54 TMZ-resistant ($D54^{Res}$) cells were generated from the D54 glioma cell line (36) and were maintained in identical media. The human cell lines were tested at the M.D. Anderson Characterized Cell Line Core Facility using short tandem repeats DNA profiling. The cell lines were free of *Mycoplasma* and pathogenic murine viruses (assayed by Scientific Applications International Co., Frederick, MD).

Antibodies and reagents

The following antibodies were titrated and used in this study: anti-CD31, anti-ET_AR (BD Biosciences, San Jose, CA); anti-ET_BR (Santa Cruz Biotechnology, Santa Cruz, CA); anti-glial fibrillary acidic protein (GFAP) (BioCare Medical, Concord, CA); anti-glutathione *S*-transferase A5 (Gsta5) (Novus Biologicals, Littleton, CO); anti-Ki67, anti-alpha smooth muscle actin (α-SMA) (AbCam, Cambridge, MA); anti-AKT, anti-phospho-AKT (Ser-473), anti-MAPK, anti-phospho-MAPK (Thr-202 and Tyr-204), anti-Twist1, anti-Bcl2L1, anti-beta-actin (Cell Signaling Technology, Beverly, MA); goat anti-rat Alexa 594, goat anti-rabbit Alexa 488, rabbit anti-goat Alexa 488, (Invitrogen, Carlsbad, CA); rabbit anti-goat FITC (Jackson ImmunoResearch Laboratories, West Grove, CA);

The selective ET_AR antagonist BQ123, selective ET_BR antagonist BQ788, TMZ [4-methyl-5-oxo-2,3,4,6,8,-pentazabicyclo[4.3.0.] nona-2,7,9-triene-9-carboxamide], and 3,3′-diaminobenzidine were purchased from Sigma-Aldrich (St. Louis, MO). Macitentan [*N*-[5-4-Bromophenyl)-6-[2-[(5-bromo-2-pyrimidinyl) ethoxy]-4-pyrimidinyl]-*N*′-

propylsulfamide] was provided by Actelion Pharmaceuticals, Ltd. (Allschwil, Switzerland). Atrasentan was purchased from Diverchim SA (Roissy-en-France, France). Zibotentan was purchased from APAC Pharmaceutical LLC (Columbia, MD).

Immunofluorescence microscopy and TUNEL assay

Sections were fixed in ice-cold acetone for 15 minutes, incubated in protein blocking solution for 20 minutes, and then at 4°C overnight with primary antibodies (1:100) in blocking solution. Control samples were incubated with corresponding IgG isotype antibodies (1:100). Samples were rinsed three times in PBS, incubated in blocking solution for 20 minutes and then incubated with corresponding secondary antibodies (1:1500) in blocking solution for 1 hour and then mounted. TUNEL was performed using a commercial apoptosis detection kit according to the manufacturer's instructions (Promega, Madison, WI). Formalin-fixed paraffin sections of clinical and experimental glioblastoma (LN-229) were processed and stained with anti-GFAP antibody (1:400). GFAP positive cells were detected with stable 3′,3′-diaminobenzidine (Research Genetics). All images were captured with an Olympus BX-51 microscope equipped with a DP71 digital camera and then processed with DP Controller and DP Manager software (Olympus America Inc., Center Valley, PA).

Chemoprotection assay

To evaluate the effect of astrocytes and brain endothelial cells on the sensitivity of LN-229 glioma cells to TMZ, we performed a series of *in vitro* chemoprotection assays, as previously described (33). In brief, murine astrocytes, endothelial cells, and 3T3 fibroblasts were transfected with GFP genes and then plated along with LN-229 glioma cells (cancer cell: test cell plating ratio of 1:2) onto individuals wells of sterile six-well dishes and allowed to stabilize overnight. In some experiments, the co-incubated cells were treated with 100 nM of type-specific endothelin antagonists, atrasentan (ET_AR), zibotentan (ET_AR), BQ123 (ET_AR), BQ788 (ET_BR), BQ123 and BQ788, or with 100 nM of the dual endothelin receptor antagonist, macitentan, for two hours before being challenged with 20 μg/ml TMZ. After 72 hours, the GFP-labeled cells were separated from LN-229 glioma cells by fluorescence-activated cell sorting and the apoptotic fraction of glioma cells was determined by propidium iodide-stained DNA, as previously described (33).

Animals

Female athymic nude mice (NCI-nu) were purchased from the Animal Production Area of the National Cancer Institute-Frederick Cancer Research Facility (Frederick, MD) and housed and maintained in specific pathogen-free conditions. The facilities are approved by the American Association for Accreditation of Laboratory Animal Care and meet all current regulations and standards of the United States Department of Agriculture, United States Department of Health and Human Services, and National Institutes of Health. The mice were used in accordance with institutional guidelines when they were 8–12 weeks old.

Orthotopic implantation of human glioblastoma cells in nude mice

Glioma cells (LN-229, LN-229Res, and D54^{Res} cells) were harvested in log-phase growth by briefly exposing glioma cell cultures to a solution containing 0.25% trypsin and 0.02% EDTA. The cells were washed and resuspended in Ca^{++}/Mg^{++}-free Hanks' balanced salt solution (HBSS). Glioblastomas were produced by stereotactically implanting either 1×10^5 cells or 2×10^5 cells in 4 μl of HBSS into the brain parenchyma of female nude mice as previously described (37).

Luciferase transfection and IVIS imaging

LN-229 cells were plated onto 24-well plates at a density of 5×10^4 cells/well in MEM containing 10% FBS and placed in a 37°C incubator overnight. Firefly luciferase lentivirus (Capital Biosciences, Rockville, MD) was diluted in MEM with polybrene (Millipore, Billerica, MA) to a final concentration of 8 μg/mL and added to each well. After an overnight incubation period, the media was replaced with polybrene-free MEM. The infected LN-229 cells were selected using puromycin (0.5 μg/mL) and individual clones were screened for luciferase activity by measuring their light emission with the Xenogen IVIS-100 system (Caliper Life Sciences, Hopkington, MA) after adding D-luciferin (150 μg/mL). Bioluminescent imaging of orthotopically implanted luciferase-labeled glioma cells was achieved by intraperitoneal injection of 150 mg/kg D-luciferin to mice. Measurements were collected on a calibrated instrument and photon flux from the tumor was monitored each week. The exposure time, F-stop, and pixel binning were optimized in Living Image software (Xenogen Corp., Alameda, CA) and the bioluminescent signal was displayed as an intensity map.

Therapy experiments

Therapy was initiated when orthotopically implanted glioblastomas were considered established (21–24 days after implantation) as determined by bioluminescent imaging analysis using the Xenogen IVIS Imaging System. TMZ was administered daily using an oral dose of 7.5 mg/kg at different schedules. Macitentan was administered daily using an oral dose of 10 mg/kg. Zibotentan was administered daily using an oral dose of 20 mg/kg, whereas atrasentan was administered daily by intraperitoneal injection at a dose of 10 mg/kg. Throughout the course of the survival studies, mice were monitored for weight loss, dehydration, and onset of any abnormal neurological signs, such as lethargy, hyperkyphosis, tilted neck, or circling. Animals that exhibited these signs were euthanized by intraperitoneal injection of 1 g/kg of nembutal. All survival durations were recorded and all brains were harvested and examined using routine histological and immunohistochemical techniques. Reconstitution formulae were 0.5% DMSO for TMZ, 0.25N $NaHCO_3$ for atrasentan, 0.5 mg/ml PBS for zibotentan, and 0.05% (wt) methylcellulose solution containing 0.05% (vol) Tween 80 for macitentan.

Western blot analysis

Western blot analyses for AKT and MAPK and their phosphorylated forms were carried out as previously described (33). LN-229 glioma cells were orthotopically implanted into brains of nude mice and twenty-one days later the mice were treated with vehicle (n=6) or 10

mg/kg macitentan (*n*=6) each day for a period of three weeks. Mice were euthanized and proteins were extracted from the glioblastomas with lysis buffer consisting of 7 M Urea, 2 M thiourea, 4% CHAPS, 1% DTT, a phosphatase inhibitor (Roche, Basil, Switzerland), and a protease inhibitor cocktail (Roche).

MGMT promoter methylation assay

We evaluated the methylation status of the *MGMT* promoter using a method previously described (38). Thirty-six female nude mice harboring three-week-old LN-229, LN-229Res, or D54^{Res} orthotopically implanted glioblastomas were randomized into the following treatment groups: vehicle, TMZ, macitentan, macitentan plus TMZ. Treatment was started 21 days following glioma cell implantation. Macitentan was administered daily, while TMZ was administered daily on a one-week-on two-weeks-off schedule. Therapy was administered for four weeks and DNA was extracted from glioblastoma tissues three hours after the final treatment.

Sodium fluorescein permeability assay

We assessed the permeability of the tumor vasculature to the fluorescent tracer sodium fluorescein (Sigma: NaFl: MW 376 Da), as previously described (39). In brief, we implanted 2×10^5 LN-229 cells into the brain parenchyma of female nude mice and then randomized the mice into 2 treatment groups: control (vehicle) (*n*=5) and macitentan (*n*=5). Tumors were allowed to develop for 21 days after which the mice were treated daily with vehicle or 10 mg/kg of macitentan for a period of two weeks. Four hours after the final dose of macitentan, the mice were injected intraperitoneally with 20 mg of NaFl in 200 μl of sterile normal saline. The NaFl was allowed to circulate for 10 minutes and then the mice were euthanized and their brains processed for frozen sections. Sections were stained for CD31 expression as described above.

Small-animal magnetic resonance imaging (MRI)

MRI monitoring to evaluate the effect of macitentan treatment on the uptake of contrast agent in orthotopically implanted LN-229 glioblastoma tumors in Swiss nude mice (Charles River, France) was performed by Oncodesign (Dijon, France). Twenty-four hours before glioma cell implantation, the mice were irradiated with a g-source (whole body irradiation, 2.5 Gy, 60Co, INRA, Dijon, France). Glioblastomas were generated as described above and 21 days days following the implantation of glioma cells, the mice were randomized into two groups and were administered vehicle (*n*=4) or 10 mg/kg macitentan (*n*=4) once daily for 21 consecutive days. Images were obtained weekly once treatment started using optimized parameters defined with and without contrast agent. Imaging was performed on a 4.7T horizontal magnet (PharmaScan, Bruker Biospin GMBH, Germany) equipped with an actively shielded gradient system. MR images were acquired using ParaVision (PV5.0, Bruker Biospin). Mice were anesthetized using 2% isoflurane and positioned supine in a mouse cradle that was inserted in a volume coil within the PharmScan. Scout images were acquired for calibration purposes and adjustments were performed to optimize shim, RF power, and amplification of the MR signal. T2 and then T1 pre-contrast images were collected and mice were administered a bolus injection of 0.2 mmol/kg gadopentetate

dimeglumine (Gd-DTPA, Magnevist, Bayer Healthcare Pharmaceuticals, Germany) through a 24-gauge catheter that was inserted in the caudal vein. Three minutes after the contrast agent was administered, T1 post-enhancement images were obtained. MR images were analyzed with ImageJ and the percentage of enhancement following contrast was calculated by voxelwise subtraction of T1 pre-signal from T1 post-signal.

Pericyte coverage and microvascular density (MVD)

To determine the extent of pericyte coverage of tumor-associated blood vessels, we stained tumor sections from each of the treatment groups with CD31 (red) and α-smooth muscle actin (α-SMA: green; Abcam, Cambridge, MA) antibodies and then with their corresponding secondary antibodies. Four fields from each section were randomly selected at a magnification of ×400, and those blood vessels that were at least 50% covered by green α-SMA-positive cells were considered to be positive for pericyte coverage.

Tumor MVD was determined as previously described (40). Brain sections from mice that had been treated with vehicle, macitentan, TMZ, or combined macitentan plus TMZ for a period of 21 days were processed for immunofluorescence microscopy and labeled with anti-CD31 antibodies and then with Alexa594 secondary antibodies. A minimum of 3 tumors from each of the treatment groups was used in the analysis and brains harvested from 3 normal (non-tumor-bearing) mice were also included in the analysis.

Statistical analysis

Statistical analyses for the chemoprotection assay, pericyte coverage, and tumor MVD were performed with Prism 6.01 (GraphPad Software, San Diego, CA) using Student's *t*-test. A P value of <0.05 was considered statistically significant. For *in vivo* studies, Kaplan-Meier survival plots were generated and comparisons between survival curves were made using the log-rank statistic.

Results

Heterogeneous expression of ET_AR and ET_BR in experimental LN-229 glioblastomas patterns their distribution in clinical tumors

We compared expression of GFAP, ET_AR, and ET_BR in LN-229 glioblastomas that were orthotopically implanted in nude mice with expression in clinical glioblastoma specimens. GFAP is the prototypical marker for immunohistochemical identification of reactive astrocytes (41). Experimental and clinical tumors were highly invasive and surrounded and infiltrated by $GFAP^+$ astrocytes (Fig. 1). ET_AR and ET_BR were heterogeneously expressed on glioma cells and tumor-associated endothelial cells in both experimental and clinical tumors.

Macitentan abolishes astrocyte- and brain endothelial cell-mediated protection of LN-229 glioma cells from TMZ

Reports suggest that astrocytes (33) and brain endothelial cells (33, 42) may contribute to treatment failure by protecting cancer cells from chemotherapy. We found that murine astrocytes and murine brain endothelial cells co-cultured with LN-229 glioma cells protected

the cancer cells from TMZ. The apoptotic index of LN-229 glioma cells co-incubated with murine astrocytes and treated with TMZ was significantly reduced in comparison to LN-229 glioma cells cultured alone in TMZ ($P<0.05$) (Fig. 2A). To determine whether astrocyte-mediated protection of glioma cells was mediated through endothelin signaling, we treated cell cultures for 2 hours with type-specific endothelin receptor antagonists BQ123 (ET_AR), BQ788 (ET_BR), BQ123 and BQ788, or with the dual antagonist, macitentan, and then further incubated the cells in TMZ. The chemoprotective effect was still observed in LN-229 glioma cells that were co-incubated with astrocytes and treated with either BQ123 or BQ788. However, treatment with both BQ123 and BQ788 or with macitentan nullified the protection.

The apoptotic index of LN-229 cells co-incubated with brain endothelial cells in TMZ was also significantly reduced when compared to LN-229 cells growing alone in TMZ ($P<0.01$) (Fig. 2B). Neither BQ123 nor BQ788 alone had any effect on brain endothelial cell-induced chemoprotection, whereas the protective effect was abolished by the combined administration of BQ123 and BQ788 or macitentan. Murine fibroblasts had no effect on the chemosensitivity of glioma cells (Fig. 2C).

Combination therapy with macitentan and TMZ produces regression of established orthotopic LN-229 glioblastomas

Next, we conducted several survival studies to test the efficacy of macitentan and TMZ in established glioblastomas in brains of nude mice (*i.e.*, therapy as opposed to prevention studies). To ensure that tumors were established before administering therapy, we labeled LN-229 glioma cells with luciferase and monitored their intracranial growth using non-invasive bioluminescence imaging. In the first study, we implanted 2×10^5 luciferase-labeled LN-229 cells into the brain parenchyma of nude mice and then randomized the mice into 4 treatment groups ($n=10$ mice/group): vehicle (control), TMZ, macitentan, and macitentan plus TMZ. TMZ was administered daily using a 7-days-on/14-days-off regimen and macitentan was administered daily. Treatment was initiated 24 days after implantation of glioma cells and the study was terminated on day 98. Macitentan therapy alone had no effect on survival. TMZ prolonged survival ($P<0.05$), but only mice that received macitentan plus TMZ were alive at the culmination of the study ($P<0.0001$, log-rank test) (Fig. 3A). We were unable to detect luminescence signals in mice that received the combination treatment and no glioblastoma cells were identified by histological analysis of brain sections. Results from the bioluminescence imaging analysis are shown in Supplementary Fig. S1. Representative gross images of coronal sections from the brains of mice harboring LN-229 glioblastomas and treated with the different therapies are shown in Supplementary Fig. S2A. The upper panel of Supplementary Fig. S2B shows a representative histologic image of a normal mouse brain and the brain of a mouse three weeks after implantation of LN-229 glioma cells. The lower panel of Supplementary Fig. S2B depicts representative images of brains from LN-229 tumor-bearing mice that received short-term (3 weeks) therapy. Representative images from the histological analysis of brain sections from mice harboring LN-229 glioma cells, as well images from mice harboring TMZ-resistant glioblastomas ($LN\text{-}229^{Res}$ and $D54^{Res}$) from later experiments, are depicted in Supplementary Fig. S2C.

In the second study, we implanted 1×10^5 luciferase-labeled LN-229 cells into the brains of nude mice (n=10 mice/group) and initiated treatment 28 days later. TMZ was administered using a dose-dense 7-days-on/7-days-off regimen. The study was terminated on day 130. Macitentan administered alone did not prolong survival. The dose-dense TMZ schedule prolonged survival in the TMZ-treated group (P<0.01), but by day 120, all mice that had received only TMZ were dead (Fig. 3B). In contrast, all mice treated with macitentan plus TMZ therapy were alive on day 130 (P<0.0001, log-rank test) and had no evidence of intracranial disease as determined by bioluminescence imaging.

Macitentan downregulates survival pathways in glioma cells and tumor-associated endothelial cells, which enhances their sensitivity to TMZ

We performed biomarker analyses on LN-229 glioblastomas from mice that were treated for a period of three weeks. TMZ was administered using the 7-days-on/7-days-off schedule. ET_AR and ET_BR were expressed on glioma cells and tumor-associated endothelial cells in all mice (Fig. 4A). The activated forms of AKT and MAPK were expressed by glioma cells and tumor vascular endothelial cells in vehicle- and TMZ-treated mice, but were deficient in tumors from mice treated with macitentan or macitentan plus TMZ. We confirmed that macitentan down-regulates expression of the phosphorylated forms of AKT and MAPK in LN-229 in orthotopically implanted glioblastomas using Western blot analysis (Fig. 4B). The anti-apoptotic proteins Bcl2L1, Gsta5, and Twist1 localized to glioma cells and tumor-associated endothelial cells in mice from control and TMZ groups, but were down-regulated in tumors from mice that received macitentan (Fig. 4C). We observed robust glioma cell division in mice treated with vehicle, TMZ alone, and macitentan alone. However, only few dividing glioma cells were present in tumors from mice treated with macitentan plus TMZ. Only mice treated with macitentan plus TMZ had large numbers of apoptotic glioma cells and apoptotic tumor-associated endothelial cells.

Macitentan plus TMZ produces durable responses; rare recurrent glioblastomas remain responsive to therapy

Next, we questioned whether mice treated with macitentan plus TMZ would remain disease-free after cessation of treatment and, if not, whether recurrent tumors would respond to additional cycles of macitentan and TMZ. Treatment commenced three weeks after the orthotopic implantation of luciferase-labeled LN-229 glioma cells into mice. TMZ was administered using the 7-days-on/14-days-off regimen. Treatment was stopped on day 98, when only those mice treated with macitentan plus TMZ were alive (P<0.0001, log-rank test) (Supplementary Fig. S3A). These mice did not exhibit signs or symptoms of a brain mass and no tumors were detected using bioluminescence imaging. We continued weekly imaging on these mice and on day 146 (48 days after cessation of therapy), 2 of 16 mice developed recurrent glioblastoma (Supplementary Fig. S3B) and were returned to therapy. One mouse died on day 167, whereas the other mouse responded well to treatment and had no evidence of detectable disease on day 181. On day 195 (97 days after cessation of therapy), a third mouse had a relapse of glioblastoma (Supplementary Fig. S3C). Therapy with macitentan plus TMZ was restarted and the disease was stable on day 302 when the mouse was euthanized.

Macitentan plus TMZ eradicates TMZ-resistant glioblastomas

To determine the efficacy of macitentan plus TMZ in treating TMZ-resistant tumors, we established the TMZ-resistant LN-229 cell line (LN-229Res) by exposing monolayers of LN-229 cells to increasing concentrations of TMZ over the course of 9 months. LN-229Res cells are approximately 4-times more resistant to TMZ when compared to LN-229 parental cells (IC_{50} 15 μg/ml *vs* IC_{50} 3.5 μg/ml, respectively). Therapy was initiated on two-week old LN-229Res brain tumors using a 1-week-on/2-weeks-off TMZ schedule. One mouse in the macitentan plus TMZ group was euthanized on day 97 due to rectal prolapse. The study was terminated on day 112 when only mice treated with macitentan plus TMZ were alive (P<0.0001, log-rank test) (Fig. 5A). Histologic examinations of the brains from mice treated with combination therapy revealed no evidence of disease (Supplementary Fig. S2C).

Next, we evaluated macitentan and TMZ in D54 TMZ-resistant (D54^{Res}) tumors. D54^{Res} glioma cells (IC_{50} 200 μg/ml) are almost 60 times more resistant to TMZ when compared to LN-229Res cells. Treatment was initiated two weeks after orthotopic implantation of D54^{Res} cells. After three weeks of therapy, three mice were randomly selected from each group, euthanized, and their brains processed for immunofluorescence studies. By day 60, all mice in the control and TMZ groups had died (Fig. 5B). Two of the eight mice that received macitentan plus TMZ also died during the study (on days 62 and 70). Six of the eight mice in the combination treatment group were still alive on day 90 when the study concluded (P<0.0001, log-rank test). These mice showed no evidence of a tumor mass on subsequent histological analysis of brain sections (Supplementary Fig. S2C).

ET_AR and ET_BR expression on D54^{Res} glioma cells and tumor-associated endothelial cells was not affected by treatment with macitentan, TMZ, or both (Supplementary Fig. S4A). Macitentan down-regulated pAKT and pMAPK in D54^{Res} tumors, whereas treatment with vehicle or TMZ alone had no effect on expression of these proteins. Bcl2L1, Gsta5, and Twist1 were expressed in glioma cells and associated-endothelial cells in vehicle- and TMZ-treated tumors, but were dramatically down-regulated in mice that received macitentan (Supplementary Fig. S4B). Tumors from mice treated with macitentan plus TMZ therapy displayed a marked reduction in cell division and enhanced apoptosis of both glioma cells and tumor-associated endothelial cells.

Selective antagonism of ET_AR has no effect on astrocyte-mediated protection of LN-229 glioma cells from TMZ in vitro or in vivo

Next, we compared the ability of macitentan to abolish astrocyte-induced chemoprotection of glioma cells with a type-selective ET_AR antagonist, atrasentan, and with the type-specific ET_AR antagonist, zibotentan. Similar to our initial analysis, the apoptotic index of LN-229 glioma cells that were co-incubated with astrocytes and cultured in TMZ was significantly reduced in comparison to LN-229 glioma cells cultured alone in the presence of TMZ (Fig. 6A). Treatment with 100 nM of macitentan eliminated the astrocyte-mediated chemoprotective effect, whereas neither 100 nM of atrasentan nor 100 nM of zibotentan decreased astrocyte-induced chemoprotection.

We performed a survival study to compare the therapeutic efficacy of combining TMZ with atrasentan or zibotentan with TMZ plus macitentan therapy. Nude mice harboring 21 day-old glioblastomas were randomized into 5 treatment groups (n=13 mice/group): control, TMZ, atrasentan plus TMZ, zibotentan plus TMZ, and macitentan plus TMZ. Three mice from the macitentan plus TMZ treatment group were randomly removed and euthanized after 3 weeks of therapy and their brains harvested for immunohistochemical studies. This time point was selected to coincide with the initial decline in bioluminescent signal observed in this treatment group and also because we were unable to locate tumors for analysis in mice that received extensive combination therapy. For comparison, we collected the brains of 3 randomly selected mice from the other treatment groups when they were euthanized due to their disease. TMZ was administered according to the 1-week-on/2-weeks-off schedule. The survival study concluded on day 120 when only mice in the macitentan plus TMZ group were alive (P<0.0001, log-rank test) (Fig. 6B). The results of this study demonstrate that the addition of atrasentan or zibotentan to TMZ does not provide a survival benefit for mice with orthotopically implanted experimental glioblastomas when compared to TMZ alone.

The immunofluorescent labeling results of dividing (Ki67) and apoptotic (TUNEL) cells in LN-229 were remarkably similar to our findings generated on $D54^{Res}$ glioblastomas. Glioma cell division was readily apparent in tumors from all mice, with the exception of mice that received macitentan plus TMZ therapy (Fig. 6C). We also noted very few apoptotic cells in tumor sections from mice that received atrasentan or zibotentan. Tumors from mice treated with macitentan plus TMZ appeared to be supported by the fewest number of blood vessels. Indeed, we observed tumor-associated endothelial cell apoptosis in tumor sections from mice in virtually all tumor sections collected from mice in the macitentan plus TMZ group.

Methylation status of the *MGMT* promoter correlates with glioblastoma resistance to TMZ

Expression levels of MGMT in glioblastomas may determine a response of the tumors to alkylating agents. Epigenetic silencing of the *MGMT* gene via promoter methylation decreases MGMT expression in tumor cells (4). Compromising the MGMT DNA repair mechanism can therefore increase chemosensitivity (43). We evaluated the *MGMT* promoter methylation status in LN-229, $LN\text{-}229^{Res}$, and $D54^{Res}$ glioblastomas that were harvested from the brains of mice that had been treated for four weeks with vehicle, TMZ, macitentan, or TMZ plus macitentan. Methylation of the *MGMT* promoter progressively decreased in GBM cells that were more resistant to TMZ (Supplementary Fig. S5). However, we did not find a correlation of methylation status of *MGMT* promoter with the therapeutic effects of TMZ, macitentan, or combined TMZ plus macitentan. For example, the *MGMT* promoter was heavily methylated in $LN\text{-}229^{Res}$ glioblastomas from TMZ-treated mice, but these mice did not have a significant survival benefit when compared with vehicle-treated mice with $LN\text{-}229^{Res}$.

Combined macitentan plus TMZ reduces the MVD of LN-229 experimental glioblastomas

Macitentan relaxes pulmonary blood vessels and is currently used for the treatment of pulmonary arterial hypertension. We studied the effects of macitentan on the vasculature of experimental glioblastomas. We first questioned whether macitentan might be affecting the permeability of tumor-associated blood vessels and noted that similar amounts of NaFl

accumulated in tumors from both vehicle- and macitentan-treated groups of mice, suggesting that macitentan had little effect on the permeability of tumor-associated blood vessels (Supplementary Fig. S6A). We also performed a series of magnetic resonance imaging (MRI) studies in which mice harboring established LN-229 gliomas were treated with vehicle or macitentan each day for a period of three weeks. Mice were imaged in weekly intervals once the treatment started for a period of four weeks using optimized imaging parameters defined with and without contrast agent. No contrast agent was observed in vehicle- or macitentan-treated tumors when the tumor bulk was less than 60 mm^3 (Supplementary Fig. S6B, upper panels). However, when the tumors exceeded 60 mm^3, both vehicle- and macitentan-treated tumors became permeable to the contrast agent (Supplementary Fig. S6B, lower panels). These results suggest that effectiveness of combined macitentan plus temozolomide therapy was not likely due to the ability of macitentan to enhance delivery of TMZ to LN-229 glioblastomas.

Next, we evaluated the maturation status of the tumor-associated blood vessels from mice harboring LN-229 glioblastomas that had been treated with vehicle, macitentan, TMZ, or macitentan plus TMZ for a period of three weeks. We used pericyte coverage as an index for vessel maturation and vessels that were at least 50% covered by pericytes were considered to be positive for pericyte coverage. We noted that approximately 80% of the blood vessels in normal brain sections were covered by pericytes, whereas only 5% of tumor-associated blood vessels were considered positive for pericyte coverage (Supplementary Fig. S6C). None of the treatments used in our study altered pericyte coverage.

Finally, we evaluated the MVD of the LN-229 glioblastomas from mice that had been treated with the different therapies for a period of three weeks. The MVD of LN-229 glioblastomas was significantly less than MVD of normal brain tissue ($P<0.0001$) (Supplementary Fig. S6D). Only combined macitentan plus TMZ therapy significantly reduced the MVD of LN-229 glioblastomas. These results are consistent with our Tunel analysis demonstrating that combined macitentan plus TMZ produced apoptosis of tumor-associated endothelial cells.

Discussion

Accumulating evidence suggests that glioma stem cells reside in a vascular niche, where they are the recipients of endothelial cell-derived signals that maintain their self-renewal properties (10), protect them from TMZ (42), and promote their expansion (10, 44). Efforts to impede tumor growth by eradicating the vascular niche have proved challenging; glioblastoma-associated endothelial cells are refractory to radiation and TMZ treatment (42), and anti-VEGF therapies increase glioma cell invasion (17). Here, we demonstrate that inactivation of the endothelin receptor signaling pathway with dual endothelin receptor antagonists, including macitentan, abolishes astrocyte- and brain endothelial cell-mediated chemoprotection of glioma cells and down-regulates survival pathways in glioma cells and associated endothelial cells. The elimination of these protective barriers renders glioma cells and their vasculature sensitive to TMZ resulting in durable responses in mice.

Previously, we reported that the collective modulation of a subset of anti-apoptotic proteins could provide an index of cancer cells sensitivity to chemotherapy (45). The results of the present study support that notion and indicate that the absence of Bcl2L1, Gsta5, and Twist1 expression in glioblastomas signifies a tumor that is susceptible to chemotherapy. Whether Bcl2L1, Gsta5, and Twist1 can serve as predictive biomarkers and identify other types of tumors that will respond to chemotherapy warrants additional testing. The observation that macitentan down-regulates these anti-apoptotic proteins in tumor blood vessels and glioma cells could be expected, given that endothelin is a known survival factor for endothelial cells (46, 47) and cancer cells (21, 24), including those of glial origin (27, 28).

While macitentan produced a profound effect on survival-related protein expression in the glioblastoma microenvironment, it had no anti-tumor activity as a single agent. This finding may help to explain the disappointing results from clinical trials of single agent endothelin receptor antagonists in cancer patients (21). For example, atrasentan produced only partial responses (8%) in a phase I trial in patients with recurrent glioblastoma (48). Combination studies of type-selective endothelin receptor antagonists with chemotherapy have also failed to demonstrate improved clinical benefit (49). Indeed, our results predict that the addition of a type-selective endothelin receptor antagonist to TMZ would not provide a benefit beyond that of chemotherapy alone. The heterogeneous expression of ET_AR and ET_BR in glioblastomas reported here, and elsewhere (27), and the finding that both ET_AR and ET_BR contribute to astrocyte- and brain-endothelial cell mediated chemoprotection of glioma cells advocate the use of a dual endothelin receptor antagonist combined with TMZ for clinical evaluation in glioblastoma. It should be noted, however, the only clinical trials evaluating a dual receptor endothelin antagonist in combination with chemotherapy have also proved unsatisfactory. In a phase 2 trial in patients with stage IV melanoma, the combination of the dual endothelin receptor antagonist, bosentan, with dacarbazine therapy had no effect on tumor progression (50). In comparison to bosentan, macitentan has a significantly lower dissociation rate and a 15-fold greater receptor occupancy half-life, which results in increased potency and sustained target blockade (51, 52). When macitentan is administered *in vivo*, it is metabolized into a major active metabolite, ACT-132577, that has a long half-life (40–65 hours in humans) and functions as a dual endothelin receptor antagonist (51, 53).

Acquired resistance to TMZ remains a major barrier for effective treatment of glioblastomas; approximately 90% of recurrent glioblastomas are refractory to additional TMZ therapy (1). One mechanism whereby glioma cells become resistant to TMZ involves the selection of pre-existing TMZ-resistant cells in the parental tumor (54). Our data suggest that combination therapy with macitentan and TMZ does not necessarily select for a drug-tolerant phenotype. In the three mice with recurrent disease following cessation of therapy, one tumor responded to additional cycles of macitentan and TMZ, while another tumor did not progress after treatment was resumed. Macitentan plus TMZ therapy also produced durable responses in almost 90% of mice with TMZ-resistant tumors. As mentioned above, the response of LN-229^{Res} tumors did not appear to related to hypermethylation of the MGMT promoter. Rather, the significant results of combined macitentan plus TMZ obtained in TMZ-resistant glioblastomas suggest that the pharmacological effects on supporting stromal cells are critical to the success of this therapy. Disruption of the communication

between endothelial cells and glioma cells, which is thought to be essential for glioma progression and survival (10, 39, 41, 55), may be responsible for the profound glioma cell death observed in our models. The escape mechanism that allowed two TMZ-resistant tumors to progress on macitentan plus TMZ therapy is an area of active investigation in our laboratory.

The results from the control groups of mice in our survival analyses are consistent with those of other investigators utilizing the LN-229 model (56). However, we are unaware of any previous study that has demonstrated durable therapeutic responses in experimental LN-229 glioblastomas. For comparison, targeted inhibition of focal adhesion kinase and insulin-like growth factor-1 receptor with a dual tyrosine kinase inhibitor increased median survival in the LN-229 glioblastoma model from 28 days in the vehicle-treated group to 47 days in the experimental arm (56). Our experience with LN-229 and D54 glioblastoma models indicates that tumor regression occurs gradually and usually becomes manifest after approximately 30–40 days of continuous treatment with macitentan plus TMZ, which may be related to the kinetics of tumor cell and endothelial cell division in glioblastoma (9). Regardless, the durable responses observed in the different glioblastoma models suggest that combination therapy with macitentan and TMZ might represent an important new therapeutic approach for the treatment of glioblastoma.

Supplementary Material

Refer to Web version on PubMed Central for supplementary material.

References

1. Wen PY, Kesari S. Malignant gliomas in adults. N Engl J Med. 2008; 359:492–507. [PubMed: 18669428]
2. Omuro A, DeAngelis LM. Glioblastoma and other malignant gliomas: a clinical review. JAMA. 2013; 310:2683–710.
3. Hochberg FH, Pruitt A. Assumptions in the radiotherapy of glioblastoma. Neurology. 1980; 30:907–11. [PubMed: 6252514]
4. Hegi ME, Liu L, Herman JG, Stupp R, Wick W, Weller W, et al. Correlation of O^6-methylguanine methyltransferase (MGMT) promoter methylation with clinical outcomes in glioblastoma and clinical strategies to modulate MGMT activity. J Clin Oncol. 2008; 26:4189–99. [PubMed: 18757334]
5. Bonavia R, Inda MM, Cavenee WK, Furnari FB. Heterogeneity maintenance in glioblastoma: a social network. Cancer Res. 2011; 71:4055–60. [PubMed: 21628493]
6. Johnson BE, Mazor T, Hong C, Barnes M, Aihara K, McLean CY, et al. Mutational analysis reveals the origin and therapy-driven evolution of recurrent glioma. Science. 2014; 343:189–93. [PubMed: 24336570]
7. Phillips HS, Kharbanda S, Chen R, Forrest WF, Soriano RH, Wu TD, et al. Molecular subclasses of high-grade glioma predict prognosis, delineate a pattern of disease progression, and resemble stages in neurogenesis. Cancer Cell. 2006; 9:157–73. [PubMed: 16530701]
8. Snuderl M, Fazlollahi L, Le LP, Nitta M, Zhelyazkova BH, Davidson CJ, et al. Mosaic amplification of multiple receptor tyrosine kinase genes in glioblastoma. Cancer Cell. 2011; 20:810–7. [PubMed: 22137795]
9. Eberhard A, Kahlert S, Goede V, Hemmerlein B, Plate KH, Augustin HG. Heterogeneity of angiogenesis and blood vessel maturation in human tumors: implications for antiangiogenic tumor therapies. Cancer Res. 2000; 60:1388–93. [PubMed: 10728704]

10. Calabrese C, Poppleton H, Kocak M, Hogg TL, Fuller C, Hamner B, et al. A perivascular niche for brain tumor stem cells. Cancer Cell. 2007; 11:69–82. [PubMed: 17222791]
11. Bao S, Wu Q, Sathornsumetee S, Hao Y, Li Z, Hjelmeland AB, et al. Stem cell-like glioma cells promote tumor angiogenesis through vascular endothelial growth factor. Cancer Res. 2006; 66:7843–8. [PubMed: 16912155]
12. Wang R, Chadalavada K, Wilshire J, Kowalik U, Hovinga KE, Geber A, et al. Glioblastoma stem-like cells give rise to tumour endothelium. Nature. 2010; 468:829–33. [PubMed: 21102433]
13. Cheng L, Huang Z, Zhou W, Wu Q, Donnola S, Liu JK, et al. Glioblastoma stem cells generate vascular pericytes to support vessel function and tumor growth. Cell. 2013; 153:139–52. [PubMed: 23540695]
14. Sonoda Y, Kanamori M, Deen DF, Cheng SY, Berger MS, Pieper RO. Overexpression of vascular endothelial growth factor isoforms drives oxygenation and growth but not progression to glioblastoma multiforme in a human model of gliomagenesis. Cancer Res. 2003; 63:1962–8. [PubMed: 12702589]
15. Jain RK, di Tomaso E, Duda DG, Loeffler JS, Sorensen AG, Batchelor TT. Angiogenesis in brain tumours. Nat Rev Neurosci. 2007; 8:610–22. [PubMed: 17643088]
16. Gilbert MR, Dignam JJ, Armstron TS, Wefel JS, Blumenthal DT, Vogelbaum, et al. A randomized trial of bevacizumab for newly diagnosed glioblastoma. N Engl J Med. 2014; 370:699–708. [PubMed: 24552317]
17. de Groot JF, Fuller G, Kumar AJ, Piao Y, Eterovic K, Ji Y, et al. Tumor invasion after treatment of glioblastoma with bevacizumab: radiographic and pathologic correlation in humans and mice. Neuro Oncol. 2010; 12:233–42. [PubMed: 20167811]
18. Kedzierski RM, Yanagisawa M. Endothelin system: the double-edged sword in health and disease. Annu Rev Pharmacol Toxicol. 2001; 41:851–76. [PubMed: 11264479]
19. Yanagisawa M, Kurihara H, Kimura S, Tomobe Y, Kobayashi M, Mitsui Y, et al. A novel potent vasoconstrictor peptide produced by vascular endothelial cells. Nature. 1988; 332:411–5. [PubMed: 2451132]
20. Stow LR, Jacobs ME, Wingo CS, Cain BD. Endothelin-1 gene regulation. FASEB. 2011; 25:16–28.
21. Rosano L, Spinella F, Bagnato A. Endothelin 1 in cancer: biological implications and therapeutic opportunities. Nature Rev Cancer. 2013; 13:637–51. [PubMed: 23884378]
22. Rosano L, Di Castro V, Spinella F, Nicotra MR, Natali PG, Bagnato A. ZD4054, a specific antagonist of the endothelin A receptor, inhibits tumor growth and enhances paclitaxel activity in human ovarian carcinoma in vitro and in vivo. Mol Cancer Ther. 2007; 6:2003–11. [PubMed: 17620430]
23. Ha NH, Nair VS, Reddy DN, Mudvari P, Ohshiro K, Ghanta KS, et al. Lactoferrin-endothelin-1 axis contributes to the development and invasiveness of triple-negative breast cancer phenotypes. Cancer Res. 2011; 71:7259–69. [PubMed: 22006997]
24. Rosano L, Cianfrocca R, Spinella F, Di Castro V, Nicotra MR, Lucidi A, et al. Acquisition of chemoresistance and EMT phenotype is linked with activation of the endothelin A receptor pathway in ovarian carcinoma cells. Clin Cancer Res. 2011; 17:2350–60. [PubMed: 21220476]
25. Salani D, Taraboletti G, Rosano L, Di Castro V, Borsotti P, Giavazzi R, et al. Endothelin-1 induces an angiogenic phenotype in cultured endothelial cells and stimulates neovascularization in vivo. Am J Pathol. 2000; 157:1703–11. [PubMed: 11073829]
26. Wu MH, Huang CY, Lin JA, Wang SW, Peng CY, Cheng HC, et al. Endothelin-1 promotes vascular endothelial growth factor-dependent angiogenesis in human chondrosarcoma cells. Oncogene. 2014; 33:1725–35. [PubMed: 23584483]
27. Egidy G, Eberl LP, Valdenaire O, Irmler M, Majdi R, Diserens AC, et al. The endothelin system in human glioblastoma. Lab Invest. 2000; 80:1681–9. [PubMed: 11092528]
28. Liu Y, Ye F, Yamada K, Tso JL, Zhang Y, Nguyen DH, et al. Autocrine endothelin-3/endothelin receptor B signaling maintains cellular and molecular properties of glioblastoma stem cells. Mol Cancer Res. 2011; 9:1668–85. [PubMed: 22013079]

29. Charalambous C, Hofman FM, Chen TC. Functional and phenotypic differences between glioblastoma multiforme-derived and normal human brain endothelial cells. J Neurosurg. 2005; 102:699–705. [PubMed: 15871513]
30. Nie XJ, Olsson Y. Endothelin peptides in brain diseases. Rev Neurosci. 1996; 7:177–86. [PubMed: 8916291]
31. Nagashima G, Suzuki R, Asai J, Fujimoto T. Immunohistochemical analysis of reactive astrocytes around glioblastoma: an immunohistochemical study of postmortem glioblastoma cases. Clin Neur Neurosur. 2002; 104:125–31.
32. Fitzgerald DP, Palmieri D, Hua E, Hargrave E, Herring JM, Qian Y, et al. Reactive glia are recruited by highly proliferative brain metastases of breast cancer and promote tumor cell colonization. Clin Exp Metastasis. 2008; 25:799–810. [PubMed: 18649117]
33. Kim SW, Choi HJ, Lee HJ, He J, Wu Q, Langley RR, et al. Role of the endothelin axis in astrocyte- and endothelial cell-mediated chemoprotection of cancer cells. Neuro-Oncol. 2014; pli:nou128.
34. Langley RR, Fan D, Guo L, Zhang C, Lin Q, Brantley EC, et al. Generation of an immortalized astrocyte cell line from H-2Kb-tsA58 mice to study the role of astrocytes in brain metastasis. Int J Oncol. 2009; 35:665–72. [PubMed: 19724901]
35. Langley RR, Ramirez KM, Tsan RZ, Van Arsdall M, Nilsson MB, Fidler IJ. Tissue-specific microvascular endothelial cell lines from H-2K(b)-tsA58 mice for studies of angogenesis and metastasis. Cancer Res. 2003; 63:2971–6. [PubMed: 12782605]
36. Bigner SH, Bullard DE, Pegram CN, Wikstrand CJ, Bigner DD. Relationship of an *in vitro* morphologic and growth characteristics of established human glioma-derived cell lines to their tumorigenicity in athymic nude mice. J Neuropathol Exp Neurol. 1981; 40:390–409. [PubMed: 7252524]
37. Li H, Alonso-Vanegas M, Colicos MA, Jung SS, Lochmuller H, Sadikot AF, et al. Intracerebral adenovirus-mediated p53 tumor suppressor gene therapy for experimental human glioma. Clin Cancer Res. 1999; 5:637–42. [PubMed: 10100717]
38. Kitange GJ, Carlson BL, Schroeder MA, Grogan PT, Lamont JD, Decker PA, et al. Induction of MGMT expression is associated with temozolomide resistance in glioblastoma xenografts. Neuro Oncol. 2009; 11:281–91. [PubMed: 18952979]
39. Zhang RD, Price JE, Fujimaki T, Bucana CD, Fidler IJ. Differential permeability of the blood-brain barrier in experimental brain metastases produced by human neoplasms implanted into nude mice. Am J Pathol. 1992; 141:1115–24. [PubMed: 1443046]
40. Weidner N, Semple JP, Welch WR, Folkman J. Tumor angiogenesis and metastasis-correlation in invasive breast carcinoma. N Engl J Med. 1991; 324:1–8. [PubMed: 1701519]
41. Eng LF, Ghirnikar RS. GFAP and astrogliosis. Brain Pathol. 1994; 4:229–37. [PubMed: 7952264]
42. Borovski T, Beke P, van Tellingen O, Rodermond HM, Verhoeff JJ, Lascano V, et al. Therapy-resistant tumor microvascular endothelial cells contribute to treatment failure in glioblastoma multiforme. Oncogene. 2013; 32:1539–48. [PubMed: 22614016]
43. Wick W, Weller M, van den Bent M, Sanson M, Weiler M, von Deimling A, et al. *MGMT* testing–the challenges for biomarker-based glioma treatment. Nat Rev Neurol. 2014; 10:372–85. [PubMed: 24912512]
44. Borovski T, Verhoeff JJ, ten Cate R, Cameron K, de Vries NA, van Tellingen O, et al. Tumor microvasculature supports proliferation and expansion of glioma-propagating cells. Int J Cancer. 2009; 125:1222–30. [PubMed: 19431144]
45. Kim SJ, Kim JS, Park ES, Lee JS, Lin Q, Langley RR, et al. Astrocytes upregulate survival genes in tumor cells and induce protection from chemotherapy. Neoplasia. 2011; 13:286–98. [PubMed: 21390191]
46. Schichiri M, Kato H, Marumo F, Hirata Y. Endothelin-1 as an autocrine/paracrine apoptosis survival factor for endothelial cells. Hypertension. 1997; 30:1198–1203. [PubMed: 9369276]
47. Cifarelli V, Lee S, Kim DH, Zhang T, Kamagate A, Slusher S, et al. FOXO1 mediates the autocrine effect of endothelin-1 on endothelial cell survival. Mol Endocrinol. 2012; 26:213–24.

48. Phuphanich S, Carson KA, Grossman SA, Lesser G, Olson J, Mikkelsen T, et al. Phase I safety study of escalating doses of atrasentan in adults with recurrent malignant glioma. Neuro-Oncol. 2008; 10:617–23. [PubMed: 18477765]

49. Fizazi KS, Higano CS, Nelson JB, Gleave M, Miller K, Morris T, et al. Phase III, randomized, placebo-controlled study of docetaxel in combination with zibotentan in patients with metastatic castration-resistant prostate cancer. J Clin Oncol. 2013; 31:1740–7. [PubMed: 23569308]

50. Kefford RF, Clingan PR, Brady B, Ballmer A, Morganti A, Hersey P. A randomized, double-blind, placebo-controlled study of high-dose bosentan in patients with stage IV metastatic melanoma receiving first-line dacarbazine chemotherapy. Mol Cancer. 2010; 9:69. [PubMed: 20350333]

51. Iglarz M, Binkert C, Morrison K, Fischli W, Gatfield J, Treiber A, et al. Pharmacology of macitentan, an orally active tissue-targeting dual endothelin receptor antagonist. J Pharm Exp Ther. 2008; 327:736–45.

52. Gatfield J, Grandjean CM, Sasse T, Clozel M, Nayler O. Slow receptor dissociation kinetics differentiate macitentan from other endothelin receptor antagonists in pulmonary arterial smooth muscle cells. PloS One. 2012; 7:1–11.

53. Sidharta PN, van Giersbergen PL, Halabi A, Dingemanse J. Macitentan: entry-into-humans study with a new endothelin receptor antagonist. Eur J Clin Pharm. 2011; 67:977–84.

54. Sun S, Wong TS, Zhang XQ, Pu JK, Lee NP, Day PJ, et al. Protein alterations associated with temozolomide resistance in subclones of human glioblastoma cell lines. J Neuro Oncol. 2012; 107:89–100.

55. Gilbertson RJ, Rich JN. Making a tumor's bed: glioblastoma stem cells and the vascular niche. Nat Rev Cancer. 2007; 7:733–36. [PubMed: 17882276]

56. Liu TJ, LaFortune T, Honda T, Ohmori O, Hatakeyama S, Meyer T, et al. Inhibition of both focal adhesion kinase and insulin-like growth factor-I receptor kinase suppresses glioma proliferation *in vitro* and *in vivo*. Mol Cancer Ther. 2007; 6:1357–67. [PubMed: 17431114]

Translational Relevance

Glioblastoma is a fatal disease and efforts to control its growth by surgery, chemotherapy, and radiation have not significantly improved clinical outcome. Previously, we reported that astrocyte- and brain endothelial cell-derived ET-1 protects cancer cells from chemotherapy by upregulating expression of anti-apoptotic proteins in cancer cells. Here, we demonstrate that dual antagonism of ET_AR and ET_BR signaling abolishes astrocyte- and brain endothelial cell-induced chemoprotection of glioblastoma cells *in vitro* and, moreover, down-regulates the expression of proteins associated with cancer cell growth and survival *in vivo* in orthotopic models of glioblastoma. Indeed, when macitentan was combined with TMZ, we observed marked apoptosis of both glioma cells and tumor-associated endothelial cells, which resulted in marked regression of glioblastomas and durable responses in different models, including those that are resistant to TMZ. This combination therapy represents an important new therapeutic approach for the treatment of glioblastoma.

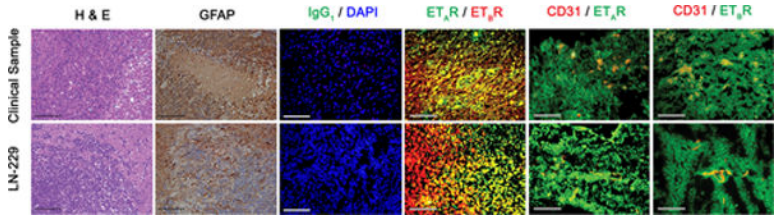

Figure 1.

Expression of ET_AR and ET_BR on tumor cells in clinical and experimental glioblastomas. LN-229 orthotopic glioblastoma pattern clinical samples in that both are invasive and infiltrated and surrounded by $GFAP^+$ reactive astrocytes. The endothelin receptors, ET_AR and ET_BR (depicted in green and red, respectively, in the middle panel, and green in other panels), are expressed on glioma cells (green) and on tumor-associated endothelial cells (red). Control samples were labeled with an IgG_1 isotype antibody. Eight clinical specimens were analyzed. A representative sample is shown. Scale bars: Black = 100 μm; White = 50 μm.

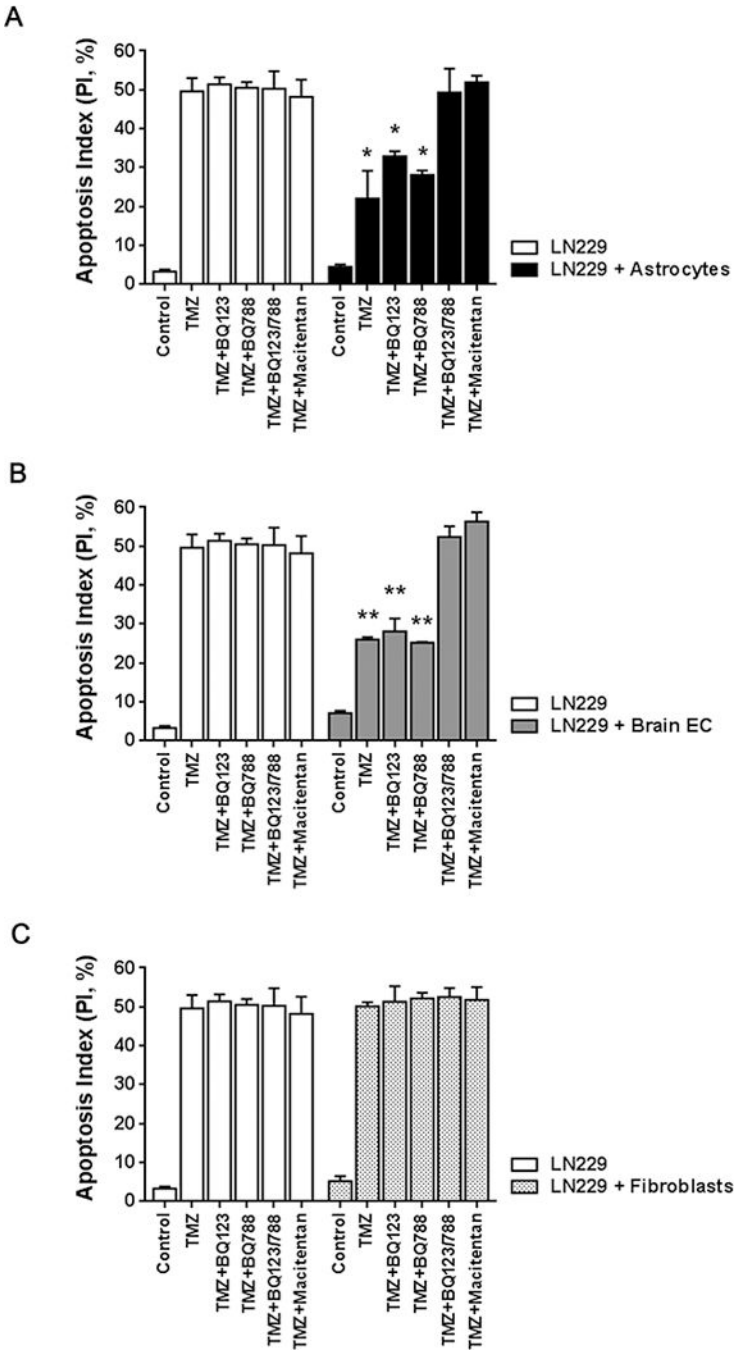

Figure 2.

Dual-antagonism of ET_AR and ET_BR abolishes astrocyte- and brain-endothelial cell-mediated protection of LN-229 glioma cells from TMZ. Comparison of the apoptotic index of LN-229 glioma cells that were cultured alone in the presence of TMZ with LN-229 glioma cells that were co-incubated with either A, murine astrocytes, B, murine brain endothelial cells, or C, murine fibroblasts, in the presence of TMZ. In some experiments, the co-incubated cells were treated with 100 nM of BQ123, BQ788, both endothelin receptor antagonists, or 100 nM of macitentan and then challenged with TMZ. Each individual single

cell test condition was compared with its corresponding co-culture condition. The data represent the mean ± s.e.m. n=3. *P<0.05; **P<0.01.

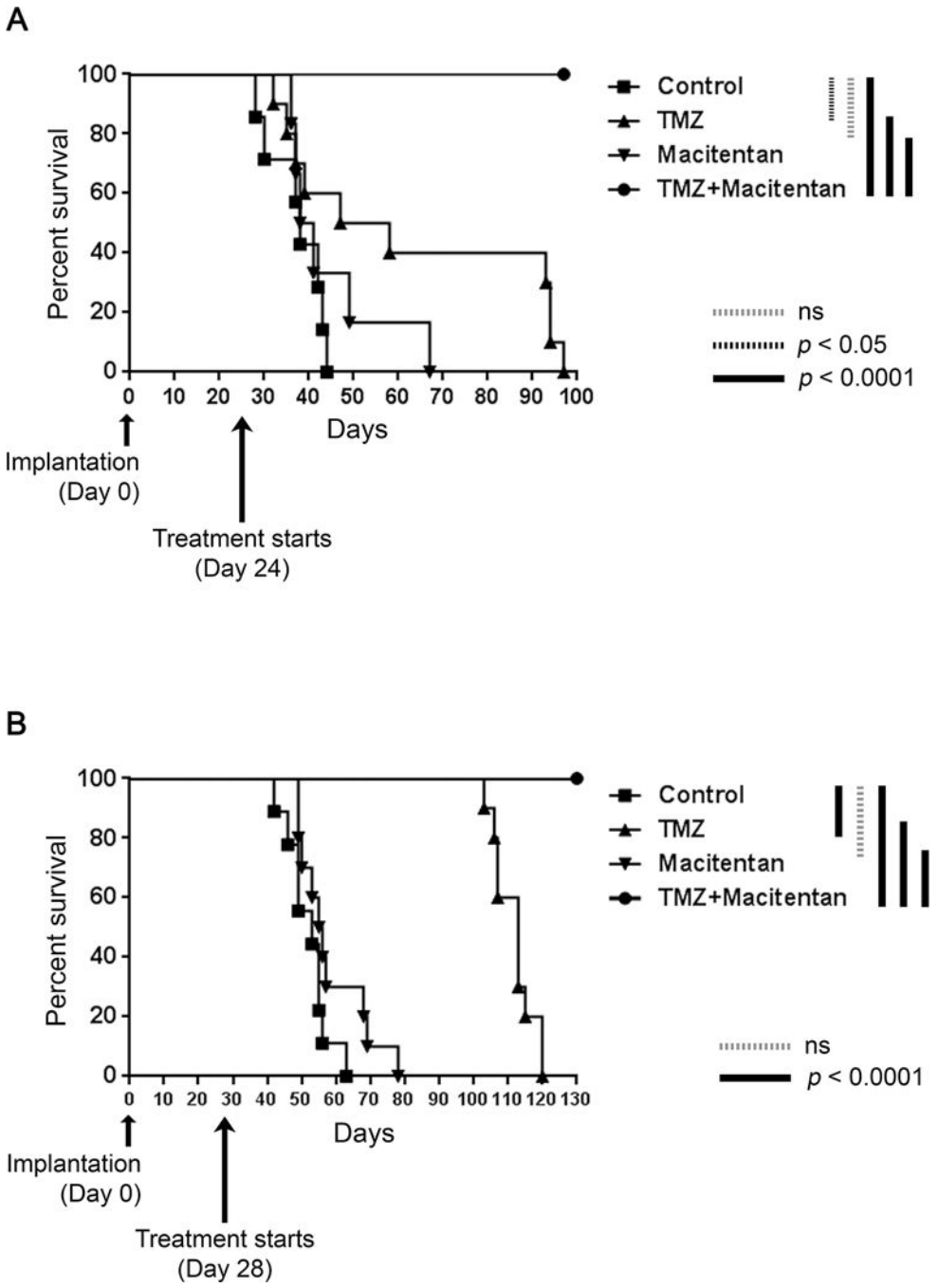

Figure 3.

Combination therapy with macitentan and TMZ significantly increases overall survival in mice with established LN-229 glioblastomas. A, Kaplan-Meier plot of mice bearing orthotopically implanted luciferase-labeled LN-229 glioma cells that were treated with vehicle (control), TMZ, macitentan, or combination therapy with macitentan plus TMZ (*n*=10 mice/group). Treatment was initiated on day 24 when tumors were established as determined by bioluminescence imaging. TMZ was administered daily using a 7-days-on/14-days-off regimen and macitentan was administered daily. B, Kaplan-Meier plot of

mice that were started on treatment four weeks after tumor cell implantation (*n*=10 mice/group). TMZ was administered daily using a 7-days-on/7-days-off regimen and macitentan was administered daily.

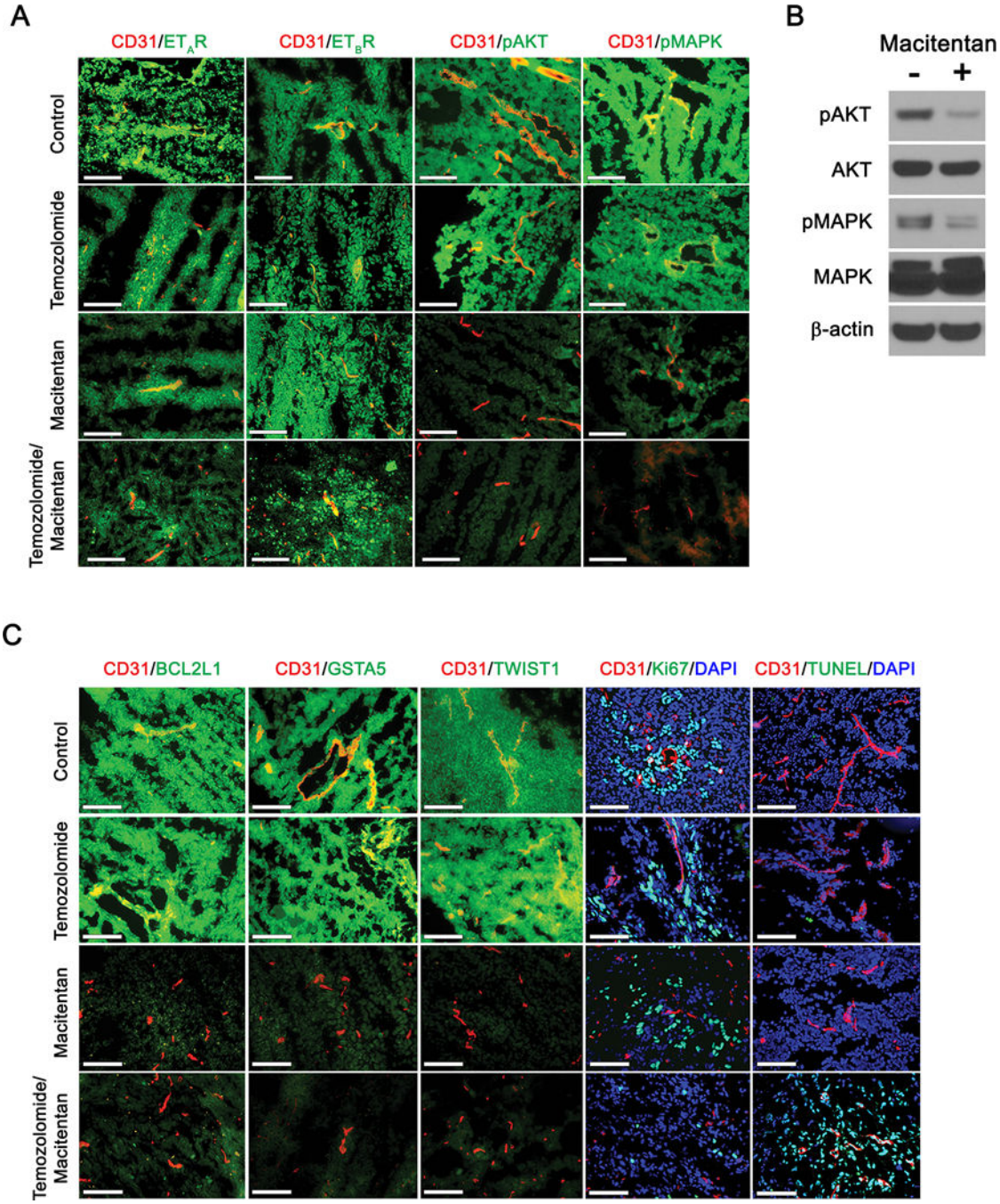

Figure 4.

Macitentan downregulates survival pathways on glioma cells and tumor-associated endothelial cells in LN-229 glioblastomas. A, Representative images from the different experimental groups after mice had received 21 days of therapy. ET_AR and ET_BR and phosphorylated AKT (pAKT) and phosphorylated MAPK (pMAPK) are depicted in green. Blood vessels were labeled with an antibody directed against CD31 (red). B, Western blot analysis of phosphorylated AKT and phosphorylated MAPK expression in orthotopically implanted LN-229 glioblastomas. Mice were treated with vehicle or 10 mg/kg macitentan

each day for a period of three weeks. C, Combination therapy with macitentan and TMZ leads to targeted destruction of glioma cells and tumor-associated endothelial cells. Representative images were collected from the different experimental groups following 21 days of therapy. Macitentan downregulates expression levels of Bcl2L1, Gsta5, and Twist1 proteins, which are labeled green. Proliferating (Ki67) and apoptotic (TUNEL) cells are also depicted in green. Blood vessels were labeled with an antibody directed against CD31 (red). Scale bar = 50 μm.

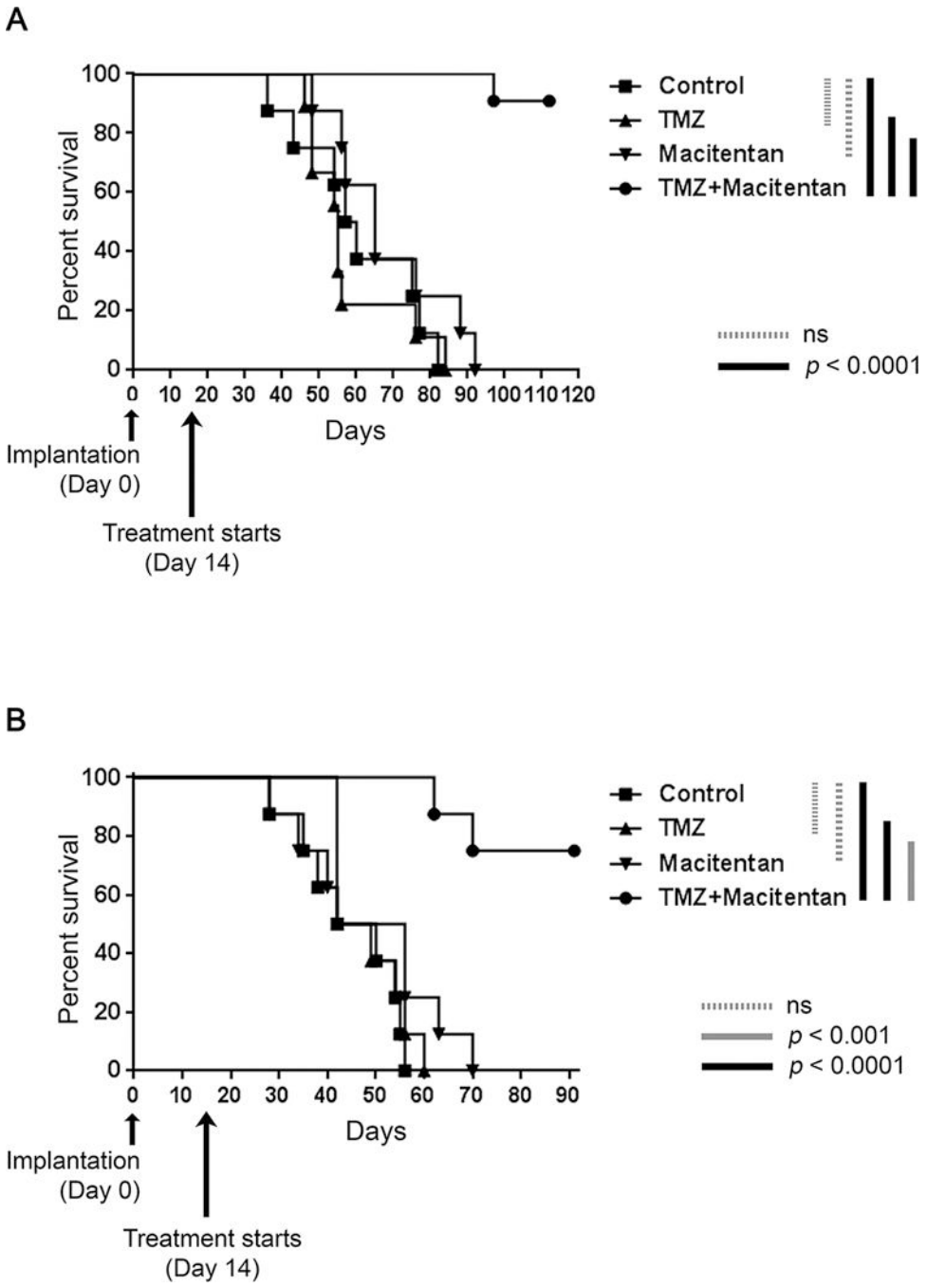

Figure 5.

Macitentan plus TMZ therapy eradicates TMZ-resistant glioblastomas. A, Kaplan-Meier plot of TMZ-resistant LN-229Res glioblastomas. TMZ-resistant LN-229Res cells (IC_{50} *in vitro* = 15 μg/ml) were implanted in the brains of nude mice and the mice were randomly assigned into 4 groups: control (*n*=8), TMZ (*n*=8), macitentan (*n*=9) and macitentan plus TMZ (*n*=10). Therapy was initiated two weeks after the orthotopic implantation of LN-229Res cells. B, Kaplan-Meier plot of TMZ-resistant D54^{Res} glioblastomas. D54^{Res} glioma cells are 57 times more resistant to TMZ (IC_{50} *in vitro* = 200 μg/ml) than parental

LN-229 glioma cells (IC_{50} *in vitro* = 4 μg/ml). Mice were randomly assigned into the 4 treatment groups (*n*=8 mice/group) and therapy was initiated two weeks later when tumors were established.

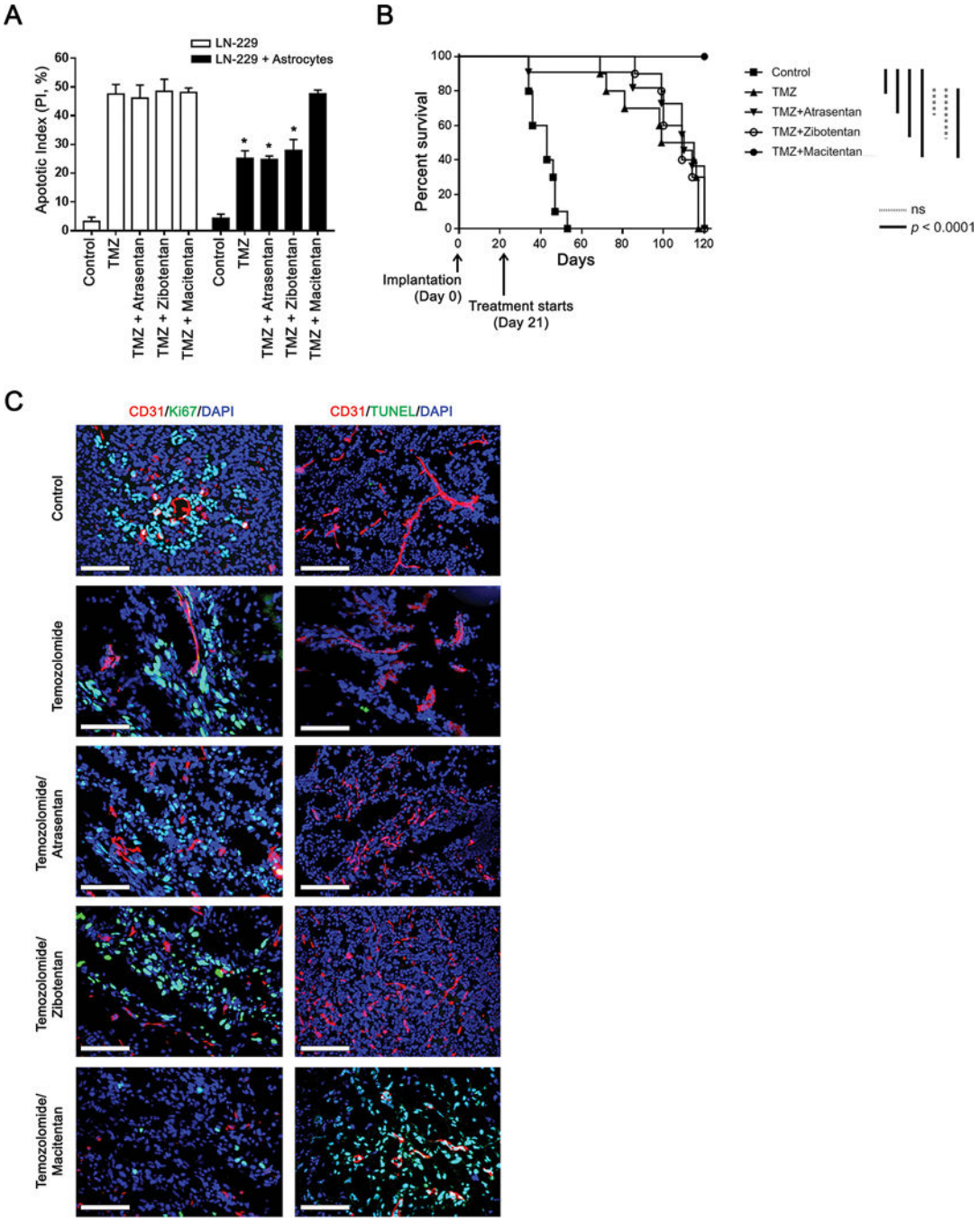

Figure 6. ET_AR antagonists alone have no effect on astrocyte-mediated chemoprotection of LN-229 glioma cells

A, Comparison of the apoptotic index of LN-229 glioma cells that were pretreated with 100 nM of the type-selective ET_AR antagonist, atrasentan, or the ET_AR type-specific antagonist zibotentan, or with 100 nM of the dual endothelin receptor antagonist, macitentan, prior to co-incubation with astrocytes. Each individual single cell test condition was compared with its corresponding co-culture condition. Each assay was conducted in triplicate with *n*=3 in each group. Statistical analysis was performed using Student's *t*-test. **P*<0.05. *Combination*

therapy with TMZ plus atrasentan or zibotentan does not provide a survival benefit when compared with TMZ alone. B, Kaplan-Meier plot of mice bearing orthotopically implanted luciferase-labeled LN-229 glioma cells that were treated with vehicle (control), TMZ, atrasentan plus TMZ, zibotentan plus TMZ, or macitentan plus TMZ (*n*=10 mice/group). Therapy was initiated three weeks after implantation of LN-229 glioma cells into the brains of nude mice. TMZ was administered using a 7-days-on/14-days-off schedule. *TMZ plus type-selective ET_AR antagonists have no effect on cell division or apoptosis in LN-229 glioblastoma microenvironment.* C, Representative immunofluorescent labeling of markers for cell division (Ki67) and apoptosis (TUNEL) in glioblastomas specimens that were collected from mice treated with vehicle (control), TMZ, atrasentan plus TMZ, zibotentan plus TMZ, or macitentan plus TMZ. Ki67 and TUNEL-positive cells are depicted in green, while blood vessels are shown in red. At least 5 photomicrographs were collected from each tumor. Scale bar=50 μm. *n*=3 mice/group.